Volume 11
Number 8
28 February 2023
Pages 2773–3132

# Journal of Materials Chemistry C

Materials for optical, magnetic and electronic devices

rsc.li/materials-c

ISSN 2050-7526

ROYAL SOCIETY OF CHEMISTRY

**COMMUNICATION**

Yuichi Kitagawa, Yasuchika Hasegawa, Kazuyuki Ishii *et al.*
A switchable system between magnetic and natural circularly polarised luminescence *via* J-aggregation using photosynthetic antenna model compounds

10 YEARS ANNIVERSARY

Journal of Materials Chemistry C

ROYAL SOCIETY OF CHEMISTRY

COMMUNICATION

View Article Online
View Journal | View Issue



Cite this: J. Mater. Chem. C, 2023, 11, 2831

Received 14th November 2022,
Accepted 13th January 2023

DOI: 10.1039/d2tc04841h

rsc.li/materials-c



# A switchable system between magnetic and natural circularly polarised luminescence *via* J-aggregation using photosynthetic antenna model compounds†

Toranosuke Tomikawa,[a] Yuichi Kitagawa,*[b] Koki Yoshioka,[d] Kei Murata,[c] Tomohiro Miyatake,[d] Yasuchika Hasegawa*[be] and Kazuyuki Ishii*[c]

**A switchable system between magnetic and natural circularly polarized luminescence *via* J-aggregation using photosynthetic antenna model compounds is demonstrated for the first time. The J-aggregation provides characteristic dispersion-type circularly polarised luminescence signals based on the degenerate J-band ($g_{CPL}$ = 0.03).**

Chiral compounds exhibit circularly polarised luminescence (CPL), which is characterized by the differential emission of right- and left-handed circularly polarised light.[1,2] CPL has attracted considerable attention because of its applications in security tags, sensors, and organic electroluminescent devices for 3D displays.[3–9]

The magnitude of CPL can be expressed using the dissymmetry factor ($g_{CPL}$).[1,2] The $g_{CPL}$ value depends on the transition electric dipole moment ($\vec{\mu}$), transition magnetic dipole moment ($\vec{m}$), and angle between $\vec{\mu}$ and $\vec{m}$. Although the combination of enhanced $|\vec{\mu}|$ and $|\vec{m}|$ offers a large $g_{CPL}$ value with bright emission, achieving this is still challenging in modern chemistry because the linear electronic motion of $\vec{\mu}$ is fundamentally different from the rotational electronic motion of $\vec{m}$. Chiral J-type aggregation is a promising strategy for achieving large $|\vec{\mu}|$ and $|\vec{m}|$ values based on the exciton chirality theory.[10–17] Ghosh *et al.* recently reported a large $g_{CPL}$ (= 4.6 × $10^{-2}$) with a high emission quantum yield ($\Phi$ = 43%) using helical J-aggregates composed of chiral naphthalene-diimide derivatives.[10] Moreover, the flexibility of aggregation can introduce switching functions. For example, Harada *et al.* have achieved flexible CPL switching behaviour using pseudo cyanine J-aggregates by thermal stimulus.[13] Using thiopheneboronic acid, Kameta *et al.* demonstrated thermal stimulus-driven CPL switching *via* morphological transformation from H- to J-aggregates ($g_{CPL}$ ≈ 0 → $g_{CPL}$ = 3.1 × $10^{-3}$).[14] Thus, flexible CPL switching systems with a large $g_{CPL}$ value can open up new possibilities for photonic applications.

Magnetic CPL (MCPL) is the CPL phenomenon under a magnetic field. MCPL is observed in both chiral and achiral compounds,[18–20] and the magnitude of MCPL for organic compounds is related to the orbital angular momentum of the aromatic π-electron system.[21,22] Specifically, the multifunction switching based on both natural CPL and MCPL is expected to provide new insights for the development of magneto-photonic materials based on polarised light.[23–25]

Herein, we provide a novel system, in which MCPL and natural CPL are switched upon J-aggregation. To demonstrate our MCPL/CPL switching concept, we employed chiral Zn-chlorin (zinc 3-devinyl-3-methoxymethyl pyropheophorbide-*a* monoester: ZnChl, Fig. 1a) with a large aromatic π-electron system because of the following reasons.[26] (1) The interaction of Zn(II) with a methoxy-substituent gives the formation of J-aggregates (Fig. 1b), which correspond to a model compound of light-harvesting antennas in green photosynthetic bacteria, *i.e.*, chlorosomes.[27] (2) The transition to the lowest excited state in the chlorin unit, called the $Q_y$ band, has a large transition probability,[28] resulting in strong light absorption and emission properties as well as good chiroptical properties in the $Q_y$ band *via* J-aggregation.[29] (3) The large orbital angular momentum derived from the large aromatic π-electron system of the chlorin unit imparts effective magneto-optical properties to the $Q_y$ band, which is weakened by the J-aggregation.[29] Based on these facts, the J-aggregation of ZnChl should be an appropriate system for realizing the switch between MCPL and natural CPL (Fig. 1c).

[a] Graduate School of Chemical Sciences and Engineering, Hokkaido University, Kita 13, Nishi 8, Kita-ku, Sapporo, Hokkaido, 060-8628, Japan
[b] Faculty of Engineering, Hokkaido University, Kita 13, Nishi 8, Kita-ku, Sapporo, Hokkaido, 060-8628, Japan
[c] Institute of Industrial Science, The University of Tokyo, 4-6-1 Komaba, Meguro-ku, Tokyo 153-8505, Japan. E-mail: k-ishii@iis.u-tokyo.ac.jp
[d] Department of Materials Chemistry, Ryukoku University, 1-5 Yokotani, Seta Oecho, Otsu, Shiga, 520-2194, Japan
[e] Institute for Chemical Reaction Design and Discovery (WPI-ICReDD), Hokkaido University, Kita 21, Nishi 10, Kita-ku, Sapporo, Hokkaido, 001-0021, Japan

† Electronic supplementary information (ESI) available. See DOI: https://doi.org/10.1039/d2tc04841h

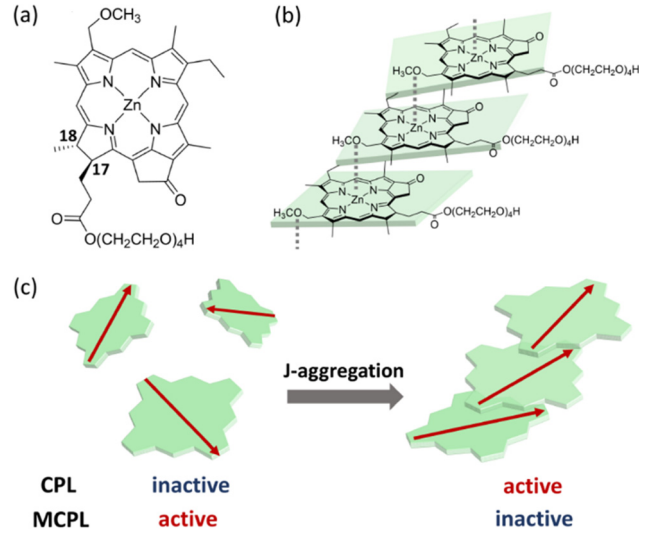


Fig. 1 (a) Molecular structure of ZnChl and (b) schematic image of the chiral J-aggregates of ZnChls.[31–38] (c) Magnetic and natural circularly polarised luminescence switching *via* J-aggregation (Red arrow: transition electric dipole moment).

ZnChl was prepared according to the previous method.[26] Here, the Zn ion was employed as the central metal ion instead of a Mg ion, since Zn chlorins are more stable than Mg chlorins.[30] The J-aggregates of ZnChls were prepared by diluting the methanol solution of ZnChl with 99-fold volume of water (ESI†).[31–38] The electronic absorption, emission, MCPL, and CPL spectra of the ZnChl monomer are shown in Fig. 2. The absorption bands at 581, 611, and 658 nm were assigned to the $Q_x(0,0)$, $Q_y(1,0)$, and $Q_y(0,0)$ bands, respectively (Fig. 2a).[29] Strong emission bands were observed at 665 and 720 nm, corresponding to their $Q_y$ bands (Fig. 2b). The emission quantum yield and lifetime were 0.067 and 4.7 ns, respectively. The $Q_y$ emission bands showed a distinguishable, positive MCPL signal (Fig. 2c, $g_{CPL}$ = 0.003) in contrast to the negligible CPL signal (Fig. 2c) derived from the poor chiroptical property of the asymmetric centre at positions 17 and 18 (Fig. 1a).

In our previous study,[29] the electronic transition bands were calculated using the time-dependent density functional theory (TD-DFT, B3LYP/6-31G(d)) method. In the calculation, we employed the structure of a ZnChl derivative having an ethyl group at position 17. The spectroscopic properties of the Q bands can be reasonably explained by Gouterman's model based on four orbitals ($b_1$, $b_2$, $c_2$, and $c_1$) and four electronic configurations (($b_1c_2$), ($b_2c_2$), ($b_1c_1$), and ($b_2c_1$)), as shown in Fig. 3a.[39,40] Because the energy difference between the ($b_2c_2$) and ($b_1c_1$) configurations is relatively large, the $Q_y$ transition mainly originates from the single electronic ($b_2c_2$) configuration (Table S1 in ref. 29). On the other hand, the ($b_1c_2$) configuration is heavily admixed with the ($b_2c_1$) configuration, resulting in weak $Q_x$ bands. Thus, with reference to the magnetic circular dichroism intensity, a strong Faraday B-type MCPL signal is observed for the $Q_y$ emission band because of the magnetic moment between the $Q_x$ and $Q_y$ bands; this magnetic moment originates from the large orbital angular momentum of the aromatic π-electron system (*i.e.*, $\langle b_2|l_z|b_1\rangle$ and $\langle c_2|l_z|c_1\rangle$).[22]

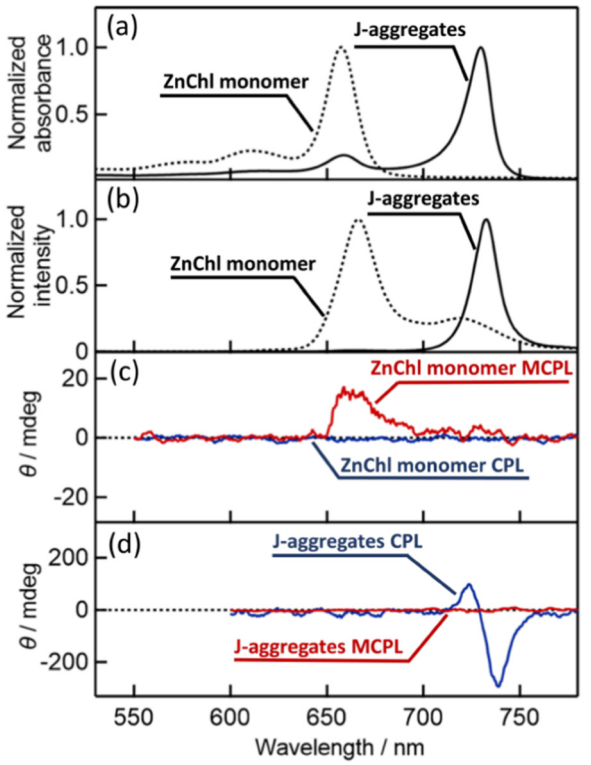


Fig. 2 (a) Electronic absorption spectra of the ZnChl monomer (dotted line) and J-aggregates of ZnChls (solid line). (b) Emission spectra of the ZnChl monomer (dotted line, $\lambda_{ex}$ = 430 nm) and J-aggregates of ZnChls (solid line, $\lambda_{ex}$ = 450 nm). (c) CPL (blue line) and MCPL (red line) spectra of the ZnChl monomer ($\lambda_{ex}$ = 430 nm). (d) CPL (blue line) and MCPL (red line) spectra of J-aggregates of ZnChls ($\lambda_{ex}$ = 450 nm).

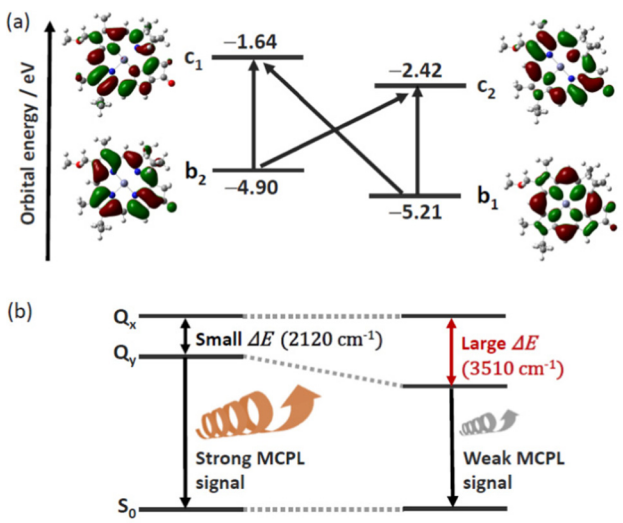


Fig. 3 (a) Molecular orbitals of ZnChl.[29] (b) Energy diagram of the ZnChl monomer and their J-aggregates for explaining the ineffective MCPL due to J-aggregation. The molecular orbitals (isosurface value = 0.02) were calculated by the DFT method (B3LYP/6-31G(d)).

 

In the electronic absorption spectrum of the chiral J-aggregates of ZnChls, the $Q_y$ band remarkably shifted to the red-side (729 nm) owing to the exciton interaction between the ZnChl units, whereas the shift of the $Q_x$ band was very small. The narrow J-band (FWHM of 280 $cm^{-1}$) reflects the formation of well-ordered J-aggregates. Consequently, the J-aggregation promotes the energy separation between the $Q_y$ and $Q_x$ bands (monomer, 2120 $cm^{-1}$; J-aggregates, 3510 $cm^{-1}$). In the emission spectrum, a sharp signal was observed at 732 nm with a small Stokes shift ($\Delta E$ = 60 $cm^{-1}$), as shown in Fig. 2b. The emission quantum yield was 0.004.[41] In the emissive J-band region, no distinguishable MCPL signal was observed, although the ZnChl monomer exhibited MCPL (Fig. 2c). This is reasonably explained by the increase in the energy gap between the $Q_x$ and $Q_y$ bands *via* J-aggregation, because the MCPL B term, which is proportional to $\mathrm{Im}((\langle Q_y|m|Q_x\rangle/(E(Q_x) - E(Q_y)))\langle S_0|\mu|Q_y\rangle\langle Q_x|\mu|S_0\rangle)$, is in inverse proportion to the energy gap, $E(Q_x) - E(Q_y)$ ($\langle Q_y|m|Q_x\rangle$: the magnetic moment between the $Q_x$ and $Q_y$ bands, $\langle S_0|\mu|Q_i\rangle$: the electric dipole moment of the $Q_i$ band, $E(Q_i)$: the $Q_i$ band energy). On the other hand, an opposite trend was observed for CPL. Whereas the ZnChl monomer exhibited negligible CPL signal, the chiral J-aggregates of ZnChls exhibited intense positive/negative CPL signals in the J-band region (Fig. 2d, $g_{CPL}$ = 0.03, positive peak: 723.5 nm, negative peak: 739 nm). The CPL spectrum is similar to the dispersion-type CD spectral pattern in the J-band region (Fig. S1, positive peak: 728.5 nm, negative peak: 735 nm, ESI†), which indicates the coexistence of the lowest excited singlet state and the nearby excited singlet state in the J-band region. The energy splitting (120 $cm^{-1}$) between these excited states is comparable to the thermal energy ($\sim$200 $cm^{-1}$), and therefore, the dispersion-type CPL spectral pattern was observed as a sum of the negative CPL from the lowest excited singlet state and the positive CPL from the thermally activated, nearby excited singlet state. Thus, using photosynthetic antenna model compounds, we successfully demonstrate the first system in which the MCPL/CPL behaviour is switched upon J-aggregation (Fig. 2c and d).

Finally, we attempted to theoretically clarify the difference in $g_{CPL}$ between the monomer and J-aggregates. $g_{CPL}$ is given by

$$g_{CPL} = \frac{I_L - I_R}{(I_L + I_R)/2} = 4\frac{\vec{\mu}\cdot\vec{m}}{|\vec{\mu}|^2+|\vec{m}|^2} \quad (1)$$

where $I_L$ and $I_R$ are the intensities of the left- and right-handed circularly polarised light, respectively. The ZnChl monomer did not show a distinguishable CPL signal because of its quite small $|\vec{m}|$. In the case of J-aggregates, the $g_{CPL}$ value is re-written using the following equations:

$$g_{CPL} = 4\frac{(\vec{\mu}_J)\cdot(\vec{m}_J)}{|\vec{\mu}_J|^2+|\vec{m}_J|^2} \quad (2)$$

$$\vec{\mu}_J = \sum_{p=1}^{n}\vec{\mu}^{(p)} \quad (3)$$

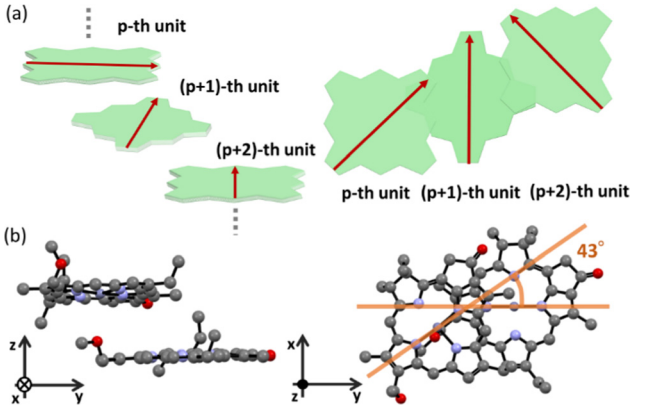


Fig. 4 (a) Schematic of ZnChl stacking (Red arrow: transition electric dipole moment). (b) The optimised structure of a ZnChl dimer. In the optimisation process, molecular mechanics (UFF) was initially used to find the energetic minimum of the dimer. Then, the geometry optimisation was calculated using the Hartree–Fock method (3-21G), followed by the DFT method (B3LYP/6-31+G(d,p)).

$$\vec{m}_J = \sum_{p=1}^{n}\vec{m}^{(p)} \quad (4)$$

Here, $\vec{\mu}_J$ and $\vec{m}_J$ are the transition electric dipole moment and transition magnetic dipole moment of the J-aggregates, respectively, and the label ($p$) denotes the $p$-th ZnChl unit in the J-aggregates (Fig. 4a). According to the exciton chirality method,[12] the $\vec{m}_J$ is expressed using the following equation:

$$\vec{m}_J = \sum_{p=1}^{n}\vec{m}^{(p)} \doteq \sum_{p=1}^{n}\left(-\frac{\omega_{na}^{(p)}}{2}\vec{r}_0^{(p)}\times\vec{\mu}^{(p)}\right) \quad (5)$$

Here, $\vec{r}_0{}^{(p)}$ and $\omega_{na}{}^{(p)}$ are the position vector and angular frequency of the transition energy for the $p$-th unit, respectively. Thus, the $|\vec{m}_J|$ value can be approximated by the $|\vec{\mu}^{(p)}|$ values, which means solving the dilemma between the linear electronic motion of $\vec{\mu}$ and the rotational electronic motion of $\vec{m}$. To obtain information about the configurations between the ZnChl units, geometry optimisation was calculated for the ZnChl dimer. In the optimisation process, molecular mechanics (UFF) was initially used to find the energetic minimum of the dimer. Then, the geometry optimisation was calculated using the Hartree–Fock method (3-21G), followed by the DFT method (B3LYP/6-31G+(d,p)). In the optimised structure, the aromatic ZnChl planes were parallel to each other, but the in-plane axes were twisted: the twisted angle was estimated to be $\sim 43^\circ$ (Fig. 4b). Based on these equations and the structural configuration, the large $g_{CPL}$ value can be reasonably explained by the twisted configuration between the ZnChl units with a large $|\vec{\mu}|$ value.

## Conclusions

Using ZnChl, the switching of MCPL/CPL *via* J-aggregation has been clearly demonstrated for the first time. The effective

exciton coupling between the ZnChl units triggers the novel switching property. These results provide new insights into the design of CPL switching materials even in solid media, and are expected to promote the development of a novel research area based on the science and technology of polarised-light.

## Author contributions

K. I. designed research. K. Y. and K. M. prepared samples. T. T., Y.K., T. M., and Y. H. performed optical measurements. T. T., Y. K., K. M., T. M., Y. H., and K. I. wrote the paper. All authors reviewed the paper.

## Conflicts of interest

There are no conflicts of interest to declare.

## Acknowledgements

This work was supported by the Institute for Chemical Reaction Design and Discovery (ICReDD), established by the World Premier International Research Center Initiative (WPI). This work was also supported by the special fund of Institute of Industrial Science, The University of Tokyo and the special fund of Research Centre for Interdisciplinary Studies in Religion, Science and Humanities, Ryukoku University.

## Notes and references

1 F. S. Richardson and J. P. Riehl, *Chem. Rev.*, 1977, **77**, 773.
2 J. P. Riehl and F. S. Richardson, *Chem. Rev.*, 1986, **86**, 1.
3 Y. Kitagawa, S. Wada, M. D. J. Islam, K. Saita, M. Gon, K. Fushimi, K. Tanaka, S. Maeda and Y. Hasegawa, *Commun. Chem.*, 2020, **3**, 119.
4 F. Zhang, Q. Li, C. Wang, D. Wang, M. Song, Z. Li, X. Xue, G. Zhang and G. Qing, *Adv. Funct. Mater.*, 2022, **32**, 2204487.
5 G. Muller, *Dalton Trans.*, 2009, 9692.
6 Y. Imai, Y. Nakano, T. Kawai and J. Yuasa, *Angew. Chem., Int. Ed.*, 2018, **57**, 8973.
7 F. Zinna, M. Pasini, F. Galeotti, C. Botta, L. D. Bari and U. Giovanella, *Adv. Funct. Mater.*, 2017, **27**, 1603719.
8 F. Song, Z. Xu, Q. Zhang, Z. Zhao, H. Zhang, W. Zhao, Z. Qiu, C. Qi, H. Zhang, H. H. Y. Sung, I. D. Williams, J. W. Y. Lam, Z. Zhao, A. Qin, D. Ma and B. Z. Tang, *Adv. Funct. Mater.*, 2018, **28**, 1800051.
9 Y. Sang, J. Han, T. Zhao, P. Duan and M. Liu, *Adv. Mater.*, 2020, **32**, 1900110.
10 A. Mukherjee and S. Ghosh, *Chem. – Eur. J.*, 2020, **26**, 1287.
11 Y. Kitagawa, H. Segawa and K. Ishii, *Angew. Chem., Int. Ed.*, 2011, **50**, 9133.
12 N. Harada and N. Koji, *Circular dichroic spectroscopy: exciton coupling in organic stereochemistry*, Tokyo Kagaku Dojin, Tokyo, 1982.
13 T. Harada, M. Kurihara, R. Kuroda and H. Moriyama, *Chem. Lett.*, 2012, **41**, 1442.
14 N. Kameta and T. Shimizu, *Nanoscale*, 2020, **12**, 2999.
15 M. Morita, D. Rau, H. Takeba and M. Herren, *Microelectron. Eng.*, 2000, **51–52**, 605.
16 M. Gon, R. Sawada, Y. Morisaki and Y. Chujo, *Macromolecules*, 2017, **50**, 1790.
17 T. Yamada, K. Nomura and M. Fujiki, *Macromolecules*, 2018, **51**, 2377.
18 R. A. Shatwell and A. J. McCaffery, *J. Chem. Soc., Chem. Commun.*, 1973, **15**, 546.
19 J. P. Riehl and F. S. Richardson, *J. Chem. Phys.*, 1976, **65**, 1011.
20 J. P. Riehl and F. S. Richardson, *J. Chem. Phys.*, 1977, **66**, 1988.
21 D. H. Metcalf, T. C. VanCott, S. W. Synder, P. N. Schatz and B. E. Williamson, *J. Phys. Chem.*, 1990, **94**, 2828.
22 J. Mack, M. J. Stillman and N. Kobayashi, *Coord. Chem. Rev.*, 2007, **251**, 429.
23 S. Pucher, C. Liedl, S. Jin, A. Rauschenbeutel and P. Schneeweiss, *Nat. Photonics*, 2022, **16**, 380.
24 N. B. Vilas, C. Hallas, L. Anderegg, P. Robichaud, A. Winnicki, D. Mitra and J. M. Doyle, *Nature*, 2022, **606**, 70.
25 P. Zhang, T. F. Chung, Q. Li, S. Wang, Q. Wang, W. L. B. Huey, S. Yang, J. Goldberger, J. Yao and X. Zhang, *Nat. Mater.*, 2022, **21**, 1373–1378.
26 T. Miyatake, S. Tanigawa, S. Kato and H. Tamiaki, *Tetrahedron Lett.*, 2007, **48**, 2251.
27 T. Miyatake and H. Tamiaki, *Coord. Chem. Rev.*, 2010, **254**, 2593.
28 S. Ogasawara, K. Nakano and H. Tamiaki, *Eur. J. Org. Chem.*, 2020, 5537.
29 Y. Kitagawa, T. Miyatake and K. Ishii, *Chem. Commun.*, 2012, **48**, 5091.
30 S. Patwardhan, S. Sengupta, F. Würthner, L. D. A. Siebbeles and F. Grozema, *J. Phys. Chem. C*, 2010, **114**, 20834.
31 Chlorophyll self-aggregates in the light-harvesting system of photosynthetic bacteria have been extensively studied, but their precise supramolecular structure has not been clarified by X-ray crystallography.[32] Balaban performed single-crystal X-ray crystallographic studies of a porphyrin-type chlorophyll model compound, which strongly supported the parallel-type supramolecular structure linked by intermolecular coordination bonds.[33] Tamiaki *et al.* reported that chlorophyll pigments without the coordinative peripheral substituent and/or central metal did not afford chlorophyll aggregates.[34] In addition, molecular modeling studies[35,36] and NMR correlation experiments[37] have supported the supramolecular structure. Thus, many studies on chlorophyllous aggregates have been discussed based on this structural model.[38] In the amphiphilic chlorophyll derivative used in this study, the presence of a coordinative methoxy group and central zinc is essential for forming the self-aggregates.[26] Consequently, the supramolecular structure shown in Fig. 1 of our manuscript is based on the widely supported structural model of the chlorophyll aggregate.

 

32 S. Matsubara and H. Tamiaki, *J. Photochem. Photobiol., C*, 2020, **45**, 100385.
33 T. S. Balaban, *Acc. Chem. Res.*, 2005, **38**, 612.
34 H. Tamiaki, M. Amakawa, Y. Shimono, R. Tanikaga, A. R. Holzwarth and K. Schaffner, *Photochem. Photobiol.*, 1996, **63**, 92.
35 A. Holzwarth and K. Schaffner, *Photosynth. Res.*, 1994, **41**, 225.
36 J. M. Linnanto and J. E. I. Korppi-Tommola, *Photosynth. Res.*, 2008, **96**, 227.
37 B.-J. van Rossum, D. B. Steensgaard, F. M. Mulder, G. J. Boender, K. Schaffner, A. R. Holzwarth and H. J. M. de Groot, *Biochemistry*, 2001, **40**, 1587.
38 V. Huber, M. Katterle, M. Lysetska and F. Würthner, *Angew. Chem., Int. Ed.*, 2005, **44**, 3147.
39 M. Gouterman, *J. Mol. Spectrosc.*, 1961, **6**, 138.
40 M. Gouterman and G. H. Wagniere, *J. Mol. Spectrosc.*, 1963, **11**, 108.
41 The emission lifetime of the chiral J-aggregates of ZnChls could not be determined because it was shorter than the instrument response function.